



*Dedicated to the memory of  
Prof. Petre T. FRANGOPOL (1933-2020)*

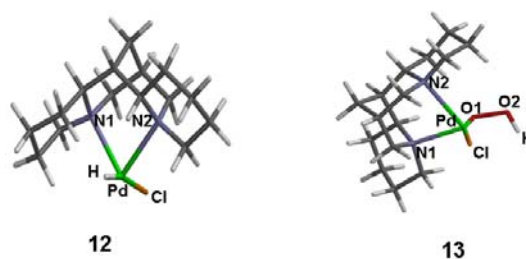
## PEROXO-TRANSITION METAL SYSTEMS: EXAMPLES OF REDOX ISOMERISM IN PALLADIUM STRUCTURES\*\*

Ioana-Alexandra SUCIU, Alexandru LUPAN and Radu SILAGHI-DUMITRESCU\*

Department of Chemistry and Chemical Engineering, “Babes-Bolyai” University, 1 Mihail Kogălniceanu str, Cluj-Napoca, RO-400084, Roumania

Received July 1, 2021

Complexes of first-row transition metals (especially iron and copper) with dioxygen, superoxide, peroxide and hydroperoxide have recently been shown to engage in complex redox isomerism phenomena, relevant to biological processes and catalysis. Such phenomena have not been discussed for heavier transition metals, which are nevertheless also known to form complexes with O<sub>2</sub> and with its partially-reduced congeners. Here, a series of palladium-peroxo, palladium-hydroperoxo, palladium superoxo or palladium-dioxygen adducts have been examined with computational methods, with emphasis on the redox isomerism phenomena. Structures computed as references include palladium-hydride complexes, where an unexpected picture of Pd-H bonding appears to emerge, suggestive of redox isomerism within the metal-hydride bond.



### INTRODUCTION

While the chemistry of palladium is dominated by the oxidation state +2, it has likewise a well-established chemistry in oxidation states ranging from 0 to +4, with some reports on +5 and +6 as well.<sup>1</sup> As such, redox isomerism appears feasible with palladium, as long as a versatile enough ligand is provided.

Oxygen activation in palladium-catalyzed processes is well known. Reaction intermediates involving dioxygen, superoxo or peroxo complexes with palladium have been invoked on a number of occasions,<sup>2-10</sup> including examination with quantum mechanical methods (density functional theory, DFT). Examples of such complexes are shown in Figure 1.

Complexes of first-row transition metals (especially iron and copper) with dioxygen, superoxide, peroxide and hydroperoxide have recently been shown to engage in complex redox isomerism phenomena, relevant to biological processes and catalysis. An example in this respect have been dioxygen binding to ferrous iron, where the redox isomers (electromers) Fe(II)-dioxygen, Fe(III)-superoxo and Fe(IV)-peroxo have been considered, with relevance to dioxygen transport (hemoglobin, myoglobin, hemerythrin) and activation (heme and non-heme oxygenases), superoxide dismutation. Electromers of the type Fe(III)-peroxo and Fe(II)-superoxo, as well as their protonated counterparts Fe(III)-hydroperoxo and Fe(II)-OOH<sup>0</sup> have also been discussed in oxygen-activating enzymes as well as in superoxide

\* Corresponding author: [radu.silaghi@ubbcluj.ro](mailto:radu.silaghi@ubbcluj.ro)

\*\* Supplementary information on <http://web.icf.ro/rrech/> or <http://revroum.lew.ro/>

dismutases and superoxide reductases. Similar redox isomerism phenomena have been investigated in related copper complexes.<sup>14-17</sup> However, no such discussion has been put forth for heavier transition metals – which are nevertheless also known to form complexes with O<sub>2</sub> and with its partially-reduced congeners.

In comparison with first-row metal peroxo complexes, the nature of Pd-O-O(H) bonding, and especially the possible redox isomerism phenomena, have received little attention. We therefore explore in the present study this redox isomerism aspect of palladium-dioxygen interaction.

## RESULTS AND DISCUSSION

The main models employed in this study are shown in Figure 1. These compounds may be seen to be grouped into different categories depending on the structure and the nature of the ligands, and were extracted from previously published computational data,<sup>2,3,10-12</sup> for all models the overall molecular charge and spin multiplicity

were taken from previously published data. Compounds **1-5** are involved into a study by Chowdhury and co-workers,<sup>10</sup> where they examined in detail the mechanism of insertion of molecular oxygen into the Pd-H bond. Compounds **6-8** and **12-13** are also involved in similar studies on oxygenations where Popp *et al.*<sup>3</sup> Compounds **9-11** were involved in a separate study by Keith *et al.* who on similar molecular oxygen insertion in a palladium<sup>II</sup>-hydride bond.<sup>2</sup> For compounds **14-15** Filatov *et al.* calculated the geometries and relative energies.<sup>11</sup> Computations on compounds **16-19** by Conley *et al.*<sup>12</sup> were focused on the reoxidation of reduced palladium species in aerobic alcohol oxidation reaction.

Energies optimized after geometry optimizations for models 1-19 are shown in Table 1. Table 2 shows optimized geometries for those models of 1-19 for which geometry optimization was successful. Figures 2-9 show these geometries, and Table 3 shows partial atomic charges derived from Mulliken population analyses.

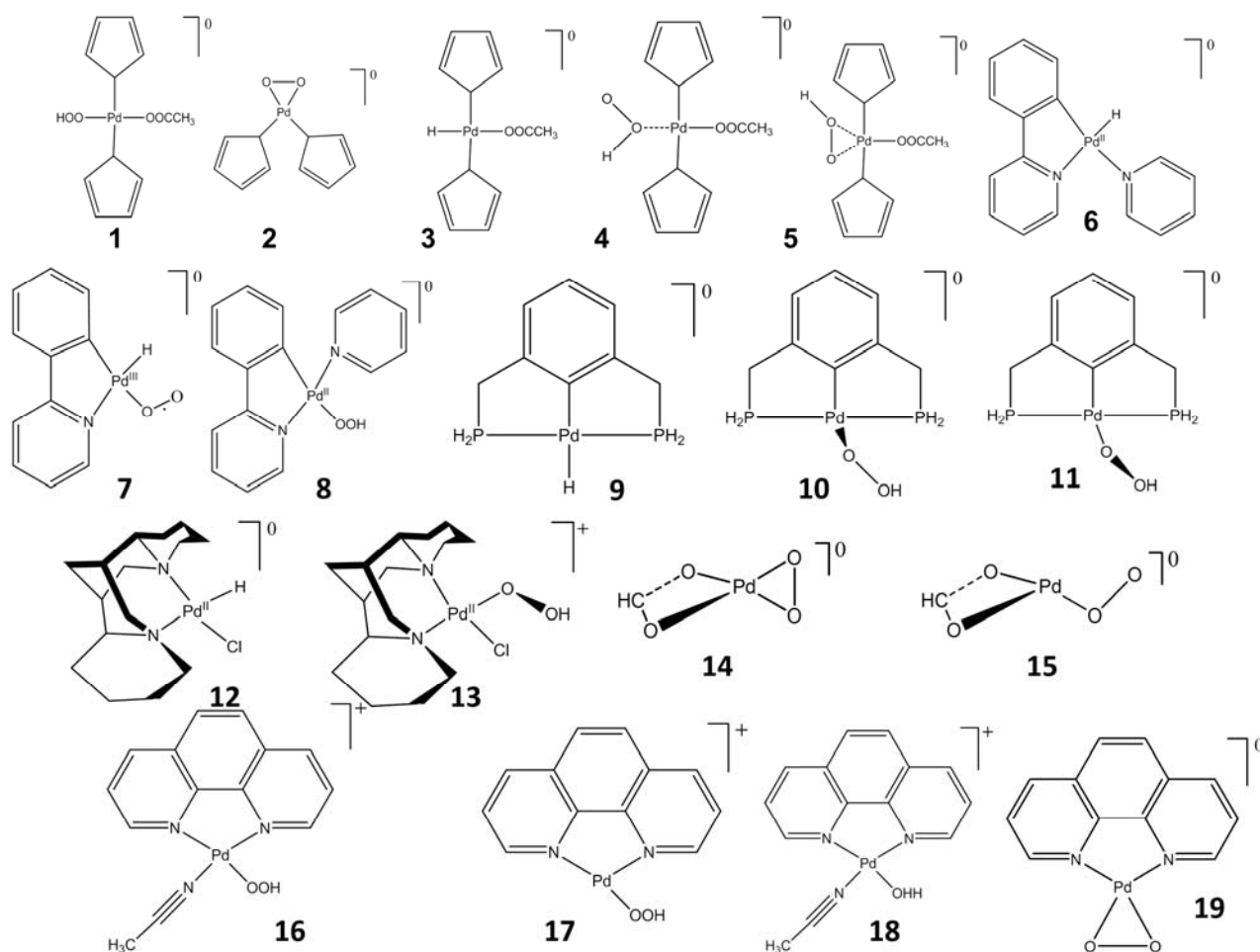


Fig. 1 – Pd-peroxo complexes of interest in the present study. “X”=H<sub>3</sub>CCOO<sup>-</sup>.<sup>2,3,10-12</sup>

Table 1

Energies (au) for models **1-23** molecules and for isolated oxygen (O<sub>2</sub>) (N.A.= not available)

Model	Energies (a.u)	Model	Energies (a.u)
1	-5706.23738	13	-6248.90126
2	N.A.	14	-5280.47999
3	-5555.79114	15	N.A.
4	-5706.19704	16	-5756.94794
5	N.A.	17	-5663.44757
6	-5668.68357	18	-5756.94794
7	-5570.67451	19	-5663.06061
8	-5819.13771	20	-356.00965
9	-5935.79264	21	-352.68719
10	N.A.	22	-348.45324
11	-6086.24945	23	-398.59835
12	-6098.66504	O <sub>2</sub>	-150.40513

The label “not available” (N/A) in Table 1 implies that an energy minimum corresponding to those particular isomers could not be located in the present work and are therefore not further discussed in text. Thus, for compound **2** geometry optimization resulted in formation of a carbon-carbon bond involving the metal-based carbons within the two ligands; this was accompanied by weakening of the Pd-C bonds. For compound **5**, a similar problem was encountered, this time involving a Pd-bound carbon atom and a Pd-bound oxygen atom belonging to the carboxylate. For model **15** (with a monodentate O<sub>2</sub> ligand), the geometry optimization led directly to a geometry identical to that of model **14** (with a bidentate O<sub>2</sub> ligand).

### 1. Energy considerations

As can be seen in Figure 1, compounds **1** and **4** are linkage isomers; Table 1 shows that **1** is more stable than **4**, by 25.3 kcal/mol. Thus, binding of OOH to the Pd is more favorable via the non-protonated oxygen – in line with previous findings on other metal-peroxo complexes.<sup>8</sup>

Compounds **9** and **11** differ by the presence of an O<sub>2</sub> moiety. The energy of **9** plus the energy of an isolated dioxygen molecular [E(**9**) + E(O<sub>2</sub>)] is higher than the energy of **11** by 32.4 kcal/mol, thus suggesting that binding of dioxygen is energetically favorable.

Compounds **12** and **13** also differ by the presence of an O<sub>2</sub> moiety. The energy of **12** plus the energy of an isolated dioxygen molecular [E(**12**) + E(O<sub>2</sub>)] is higher than the energy of **13** by

105.9 kcal/mol, thus suggesting that binding of dioxygen is very much energetically favorable.

A comparison of the energies of compounds **17** and **19** reveals that the gas-phase proton affinity of **19** is 242.8 kcal/mol, relatively small compared to what is calculated for similar iron compounds.<sup>18-21</sup>

### 2. Redox isomerism in series 1-5

For discussing redox isomerism in complexes of transition metals with redox-active diatomic ligands, it is tempting to use population analyses (some of which are nowadays particularly accurate)<sup>18</sup> and discuss partial atomic charges and spin densities. We have, however shown on a series of related models featuring Fe-O-O and Fe-N-O moieties, that the O-O and N-O bond lengths were more reliable indicators of the electronic structure in electromeric systems, particularly insofar as they were essentially insensitive to the choice of functional – whereas population analyses were seen to show significant qualitative differences depending on the choice of functional. Such dependence on the functional was especially evident in diamagnetic complexes in which one of the electromers involved an open-shell singlet with antiferromagnetic coupling; indeed, population analyses based on non-hybrid functional tend to completely ignore the open-shell contribution, even in cases where geometry clearly suggests otherwise. Solvation was also shown to affect population analyses, while having modest effects on O-O and N-O bond lengths.<sup>18</sup> It is for these reasons that in the present study, where a number of diamagnetic Pd-O-O(H) complexes are computed, we mainly rely on the O-O bond length

as a probe of redox isomerism – even though we also discuss charges derived from population analyses; moreover, also based on lessons learned from reference,<sup>18</sup> spin densities are not discussed for singlet systems, as DFT-derived spin densities were shown to be unreliable in such cases.

In models **1-5** there are two monodentate cyclopentadienyl ligands. The Pd-C bonds of models **1, 3** and **4**, at  $\sim 2 \text{ \AA}$ , are typical of metal-carbon bonds. The Pd-carboxylate bonds (Pd-O3, Pd-O4) are similar to each other and typical of a bidentate carboxylate ligand (2.2-2.3  $\text{ \AA}$ , cf. Table 2). The Pd-O<sub>2</sub>H bonds in models **1** and **4** are very similar to those computed for Fe-OOH and Fe-O(H)O adducts in other occasions.<sup>19</sup> These similarities include the fact that the Pd-O1 and

Pd-O2 bonds are different from each other by  $\sim 1 \text{ \AA}$ , and the fact that Pd-O1 is longer by  $\sim 0.2 \text{ \AA}$  in model **3** than in model **1**.

For model **1**, two electromers are possible: Pd(II)-OOH<sup>-</sup> and Pd(I)-OOH<sup>0</sup>. The O-O bond in the Pd-OOH model **1** is, at 1.42  $\text{ \AA}$ , half way between the 1.48  $\text{ \AA}$  computed at the same level of theory for H<sub>2</sub>O<sub>2</sub> and the 1.35 computed for free OOH. The sum of partial atomic charges on the OOH ligand is very close to 0 (cf. Table 3), suggesting an OOH<sup>0</sup> and hence Pd(I).

For model **4**, the O-O bond is shorter, at 1.38  $\text{ \AA}$ , and suggestive of an important contribution from the Pd(I)-superoxide. The sum of partial atomic charges on the OOH is again very close to zero, supporting this description of OOH<sup>0</sup> for the ligand.

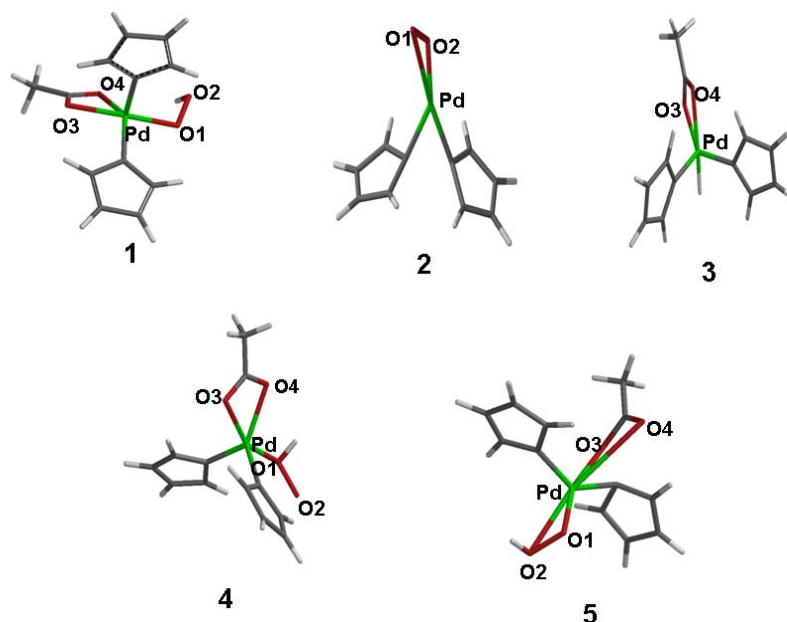


Fig. 2 – Optimized geometries for models 1-5.

Table 2

Calculated bond lengths between O-O and Pd-X (X= O, N, C, H and P) and for some reference compounds ( $\text{ \AA}$ )

Nr.	Pd-O1	Pd-O2	Pd-O3	Pd-O4	O1-O2	Pd-N	Pd-C	Pd-H	Pd-P	Pd-Cl
<b>1</b>	2.04	2.80	2.33	2.19	1.42	-	1.97	-	-	-
<b>3</b>			2.30	2.23	-	-	1.96	1.56	-	-
<b>4</b>	2.26	3.29	2.27	2.28	1.38	-	1.97	-	-	-
<b>6</b>	-	-	-	-	-	2.20	2.03	1.60	-	-
<b>7</b>	2.16	3.07	-	-	1.25	2.22	2.04	-	-	-
<b>8</b>	2.10	2.97	-	-	1.48	2.10	2.06	-	-	-
<b>9</b>	-	-	-	-	-		2.14	1.66	2.30	-
<b>11</b>	2.08	2.94	-	-	1.48	-	2.12	-	2.33	-
<b>12</b>	-	-	-	-	-	2.33	-	1.56	-	2.42
<b>13</b>	2.04	2.51	-	-	1.42	2.28	-	-	-	2.36

Table 2 (continued)

<b>14</b>	2.08	2.08	2.15	2.15	1.29	-	-	-	-
<b>16</b>	2.02	2.82	-	-	1.43	2.12	-	-	-
<b>17</b>	1.98	2.80	-	-	1.42	2.12	-	-	-
<b>19</b>	2.03	2.04			1.37	2.14	-	-	-
<b>18_Pd1</b>	-	-	2.50	-	-	2.19	-	-	-
<b>18_Pd2</b>	-	-	2.18	-	-	2.07	-	-	-
H <sub>2</sub> O <sub>2</sub>	-	-	-	-	1.48	-	-	-	-
HO <sub>2</sub> <sup>-</sup>	-	-	-	-	1.57	-	-	-	-
HO <sub>2</sub>	-	-	-	-	1.35	-	-	-	-
O <sub>2</sub> <sup>-</sup>	-	-	-	-	1.38	-	-	-	-
O <sub>2</sub>	-	-	-	-	1.23	-	-	-	-

Table 3

Charge to the Pd and some of atoms bonded to Pd (O, OOH)

Nr	Pd	O1	O2	H <sup>a</sup>	OO(H)	O3	O4	H <sup>b</sup>
<b>1</b>	0.47	-0.32	-0.22	0.33	-0.07	-0.47	-0.46	-
<b>3</b>	0.33	-0.47	-0.48	-	-0.47	-	-	0.08
<b>4</b>	0.43	-0.18	-0.31	0.37	-0.04	-0.48	-0.44	-
<b>6</b>	0.10	-	-	-	-	-	-	-0.09
<b>7</b>	0.06	0.04	0.03	-	0.03	-	-	-0.07
<b>8</b>	0.35	-0.44	-0.31	0.30	-0.15	-	-	-
<b>9</b>	-0.11	-	-	-	-	-	-	-0.10
<b>11</b>	0.07	-0.42	-0.31	0.30	-0.14	-	-	-
<b>12</b>	0.18	-	-	-	-	-	-	-0.04
<b>13</b>	0.43	-0.33	-0.19	0.36	-0.09	-	-	-
<b>14</b>	0.50	-0.10	-0.10	-	-0.10	-0.43	-0.43	-
<b>16</b>	0.48	-0.34	-0.23	0.33	-0.12	-	-	-
<b>17</b>	0.54	-0.31	-0.19	0.34	-0.05	-	-	-
<b>18_Pd1</b>	0.35	-0.53	-	0.32	-0.21	-	-	-
<b>18_Pd2</b>	0.54	-0.5	-	0.37	-0.13	-	-	-
<b>19</b>	0.44	-0.28	-0.28	-	-0.28	-	-	-

<sup>a</sup> charge to the H bonded to O; <sup>b</sup> charge to H bonded to Pd

### 3. Redox isomerism in series 6-8

In models **6-8** the Pd-N and Pd-C bonds at ~ 2.0-2.2 Å, are typical for the metal-carbon and metal-nitrogen bonds.<sup>19-21</sup> In model **7**, the Pd-oxygen distances are asymmetric, as the O<sub>2</sub> is bound to Pd in a monodentate fashion (also illustrated in Figure 8). The Pd-O1 bond in **7** is one of the weakest Pd-dioxygen/peroxo/superoxo bonds examined in the present study (2.16 Å, which is ~0.15 Å longer than most of the other Pd-O1 bonds). As the total charge of model **7** is zero, and there are two anionic ligands (hydride and

carbon), one expects that the O<sub>2</sub> ligand is electrically neutral, and bound to Pd(II). It may be surprising at first sight that the Pd(II)-O<sub>2</sub> bond is much weaker than with, *e.g.*, iron (indeed, low-spin Fe(II)-O<sub>2</sub> is ~1.75 Å).<sup>18</sup> However, it was previously shown that with the more closely-related Ni, the Ni(II)-O<sub>2</sub> bond is also very long (~2.2 Å). The reason for this difference in bond strengths is that in Pd-O<sub>2</sub> the metal has two extra d electrons in a π\* anti-bonding orbital, which makes the Fe-O bond order 1 in the palladium complex compared to 2 in Fe(II)-O<sub>2</sub> (Figure 4).

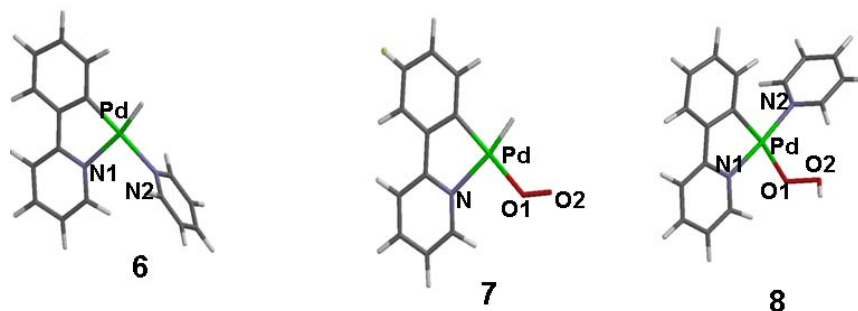


Fig. 3 – Optimized geometries for models 6-8.

The O-O bond length in model 7, at 1.25 Å, is very close to that of free O<sub>2</sub> (cf. Table 2), in very good agreement with the other data discussed above for this model, concurring towards a Pd(II)-O<sub>2</sub> description for 7, without indication of an important role for the putative Pd(III)-O<sub>2</sub><sup>-</sup> electromer – very much unlike the situation seen with earlier transition metals (Fe(II)-O<sub>2</sub>, Co(II)-O<sub>2</sub>).<sup>18</sup> The partial atomic charges computed for the O<sub>2</sub> ligand (cf. Table 3) are indeed very close to zero, as expected for O<sub>2</sub><sup>0</sup>.

In model 8 the O-OH bond length is 1.48 Å, identical to what is seen in free H<sub>2</sub>O<sub>2</sub> at the same level of theory, which implies a hydroperoxide ligand bound to Pd(II), without evidence for an important contribution from the alternative electromer, Pd(I)-OOH<sup>0</sup>.

#### 4. Redox isomerism in series 9-11

The optimized geometries for compounds 9-11 are shown in Figure 5; these three models have in common two phosphines and 10 and 11 have one hydroperoxide. The Pd-O bond distance in hydroperoxide of 2.08 Å is consistent with those of similar species.<sup>2</sup> The O-O bond length of 1.48 Å is what would be expected for a normal O-O single bond,<sup>2</sup> and thus implies again a clean Pd(II)-hydroperoxo description, similar to model 8.

#### 5. Redox isomerism in series 12-13

In compound 13 the Pd-O bond is again in the expected range and similar to the related models in Table 2 (2.04 Å); however the O-O bond length of 1.42 Å is much shorter than in models 10 and 8, and is in fact exactly midway between the O-O bonds computed for free H<sub>2</sub>O<sub>2</sub> and HO<sub>2</sub> at the same level of theory. This, together with the fact that the overall charge on the OOH ligand is only slightly below zero, suggests that in model 13 there is a significant contribution from the Pd(I)-superoxo electromer.<sup>2,22</sup> One possible reason why 13 is so different compared to the other Pd-OOH models in the present work is that the Pd in 13 is not coordinated in the square planar manner preferred by Pd(II), due to steric conflicts between the chelating ligand, the chloride and OOH.

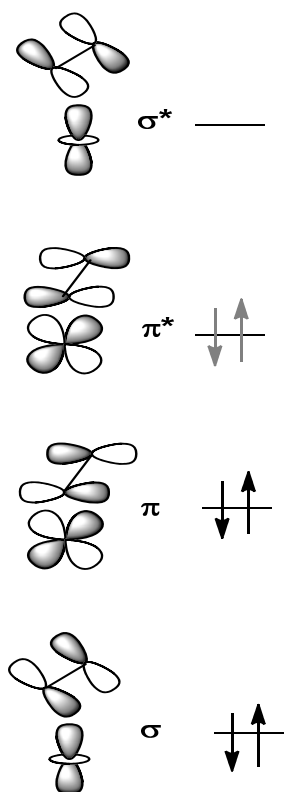


Fig. 4 – The electrons distributed in orbitals for the iron-dioxygen and nickel-dioxygen interaction. Shown in grey are the two extra electrons present in the nickel (and palladium) complexes, compared to the iron complex.

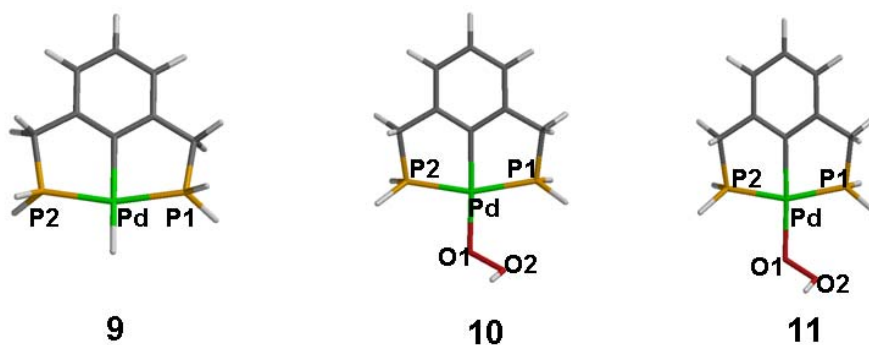


Fig. 5 – Optimized geometries for models 9-11.

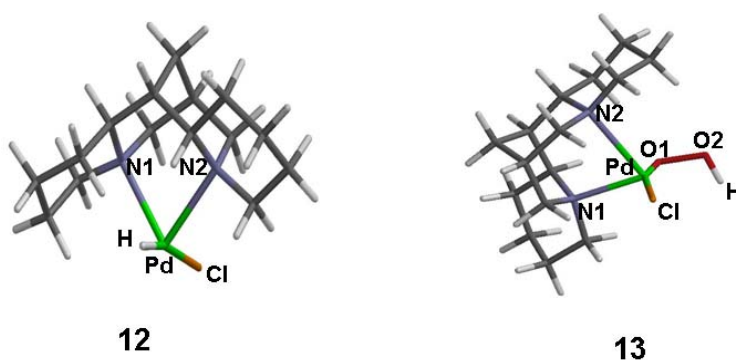


Fig. 6 – Optimized geometries for models 12-13.

### 6. Redox isomerism in series 14-15

In compound **14** the data is in good agreement with previous calculations.<sup>11</sup> The O-O distance in **14** is 1.29 Å, exactly half way between those calculated for free O<sub>2</sub> and OOH molecules, respectively. This implies that the Pd-O<sub>2</sub> moiety is half-way in between Pd(II)-OO<sup>-</sup> and Pd(I)-OO<sup>0</sup>. Table 4 shows spin densities computed for **14**; the 0.94 spin units seen on the O<sub>2</sub> ligand are very close to the value of 1 expected for a superoxide ligand, and far from the value of 2 expected for a neutral oxygen ligand. There is thus a contrast between the electronic structure predictions afforded by geometry and spin densities, respectively.

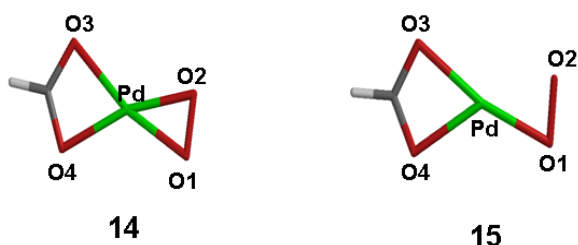


Fig. 7 – Optimized geometries for models 14-15.

The bond lengths in the hydroperoxo complexes **16-17** include an expected<sup>2,22</sup> ~2 Å for the Pd-O and 1.42-1.43 Å for the O-O bond length.

Thus, **16** and **17** are very similar to **13** in terms of O-O bond length. However, the coordination geometry around Pd in **16** and **17** is planar, suggesting that changes between tetrahedral and planar coordinations are not a factor leading to favoring of the Pd(I)-OOH electromer.

Table 4

Spin densities			
Nr.	O1	O2	Pd
<b>14</b>	0.49	0.49	0.06
<b>18_PdI</b>	0.02		0.68

### 7. Redox isomerism in series 16-19

In compound **19** the Pd-O bond length of ~2.04 Å is in line with others seen in the present study, while the O-O distance of 1.37 Å is the longest seen in non-protonated dioxygenic ligands examined by us; this value is essentially identical to those computed for free superoxide, either protonated or not, and clearly ~1 Å shorter than in free H<sub>2</sub>O<sub>2</sub> (as seen in Table 2). This suggests a strong contribution from a Pd(I)-superoxo electromer. Table 3 shows that the charge on the O<sub>2</sub> ligand in model **19** is -0.28, double compared to



other charges on formally monoanionic OOH-ligands. The computed charge on Pd is half-way between the values computed in the reference

model 18 for the Pd(I) and Pd(II) states, respectively. These data confirm a contribution from the Pd(II)-peroxo isomer.

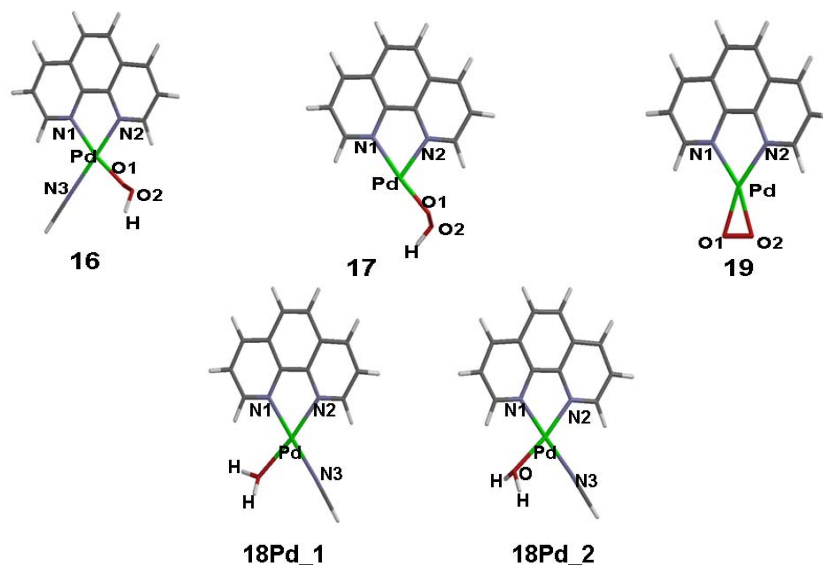


Fig. 8 – Optimized geometries for models 16 - 19.

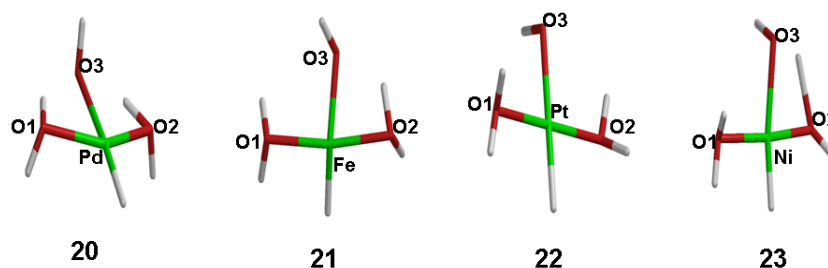


Fig. 9 – Optimized geometries for models 20-23.

### 8. Redox isomerism in the palladium-hydride bond

Structures computed as references for the dioxygen/peroxo/superoxo complexes discussed in the present work also include some palladium-hydride complexes. In general, hydride ligands are known to display remarkable variation in structure and reactivity,<sup>23</sup> with importance as key intermediates in a number of metal-catalyzed reactions.<sup>24</sup> Typical M–H distances are 1.45 to 1.6 Å for first-row elements, 1.6 to 1.7 Å for the second row, and 1.65 to 1.75 Å for the third row. Early transition metals have M–H distances about 0.1 Å longer than seen for late metals.<sup>23</sup> Also very common are the bridging hydrides.<sup>25</sup>

Compounds **3**, **6**, **9** and **12** feature palladium-hydrogen bond lengths of 1.56-1.66 Å, as expected. However, some of the charges on the hydrogens are very close to zero (*e.g.* -0.04 in

model **12**) and one is even positive: +0.08 in model **3**. In order to explore such charges in a series of simpler reference models, structures **20-23** (Figure 9) seek a comparison between a few transition metals in a simpler coordination environment (aqua ligands, with one hydroxide in order to maintain overall neutral charges).

In Table 5 the atomic charges for the models **20-23** are shown, while geometries are shown in Table 6. Metal-H bond lengths range between 1.47 and 1.80 Å as expected.<sup>2</sup> Table 5 shows that although the Pt complex shows a negative charge on the hydride as expected, and to some extent the iron compound does the same, nickel and palladium behave differently. In fact, in agreement with the data seen on model **3**, in the simple Pd model **20** the charge on the ‘hydride’ is 0.00. This cannot be an artifact of a high overall charge on the model, as the total charge is zero. We therefore propose that the Pd and to some extent even the



Ni-hydrogen bonds involve redox isomerism, with significant contribution from the electromer featuring a neutral hydrogen atom as ligand to the metal. Interestingly, Ni, as well as iron (which also features a very small charge on the hydride) are the metals used in biology at the active sites of hydrogenases, where transformations between  $H^+$ ,  $H^0$  and  $H^-$  are required as part of the catalytic cycle linking  $H_2$  and protons.

### Methodology

All models were constructed within the Builder module of the *Spartan*<sup>13</sup> package. The geometries for models **1-19** were optimized at the DFT level in the *Spartan* package, using the BP86 functional, with the gradient-corrected exchange functional proposed by Becke (1988), the correlation functional by Perdew (1986), and the DN\*\* numerical basis set (comparable in size to 6-31G\*\*). Charges and spin densities were derived from Mulliken population analyses after DFT geometry optimization.

Not shown in Figure 1 are relatively simpler structures with one central metal (Pd, Fe, Pt, Ni), two neutral water ligands, one hydride and one hydroxyl group, which served mainly as controls needed to better understand hydride binding in

some of the other models. For these, geometries and charges were computed within the Gaussian 09 software package<sup>26</sup> using the same functional, UBP86/6-31G\*\*.

### CONCLUSIONS

A series of palladium-peroxo, palladium-hydroperoxo, palladium superoxo or palladium-dioxygen adducts have been examined with computational methods, with emphasis on the redox isomerism phenomena. The data suggests that an apparent continuum of structures exist, featuring varying contributions from Pd(II)-dioxygen to Pd(III)-superoxo, from Pd(II)-peroxo to Pd(I)-superoxo, and from Pd(II)-hydroperoxo to Pd(I)-superoxide – very much like in related iron and copper complexes more widely discussed in bioinorganic chemistry. Structures computed as references include some palladium-hydride complexes, offering an unexpected picture of Pd-H bonding, different from that of most metals and suggestive of a previously undescribed redox isomerism phenomenon involving the metal-bound hydride.

*Acknowledgements.* Financial support from the Romanian Ministry for Education and Research grants PCCE 140/2008 and PN-III-P4-ID-PCE-2016-0089 is gratefully acknowledged.

Table 5

Charges of some metals (Pd, Pt, Fe, Ni) in bonding with hydrogen

Structure	20	21	22	23
Atoms	Pd	Fe	Pt	Ni
H	0.00	-0.10	-0.39	-0.03
Metal	0.10	0.21	0.04	0.07

Table 6

Calculated bond lengths between metal and oxygen, metal and hydrogen for compounds **20-23**. O1 and O2 are the oxygen atoms directed to the water, and O3 is the oxygen atom closest to the hydroxide. The last column represents the direct bonding between metal and hydrogen

Nr	Metal	Me-O1	Me-O2	Me-O3	Me-H
20	Pd	2.20	2.19	2.16	1.58
21	Fe	2.03	2.03	1.89	1.54
22	Pt	2.10	2.10	2.10	1.8
23	Ni	1.97	2.09	1.83	1.47

## REFERENCES

1. E. R. Jamieson and S. J. Lippard, *Chem. Rev.*, **1999**, *99*, 2467-2498.
2. J. M. Keith, R. P. Muller, R. A. Kemp, K. I. Goldberg, W. A. Goddard and J. Oxgaard, *Inorg. Chem.*, **2006**, *45*, 9631-9633.
3. B. V. Popp and S. S. Stahl, *J. Am. Chem. Soc.*, **2007**, *129*, 4410-4422.
4. M. M., Konnick, I. A. Guzei and S. S. Stahl, *J. Am. Chem. Soc.* **2004**, *126*, 10212-10213.
5. S. S. Stahl, J. L. Thorman, R. C. Nelson and M. A. Kozee, *J. Am. Chem. Soc.*, **2001**, *123*, 7188-7189.
6. W. R. Thiel, *Angew. Chem., Int. Ed.*, **1999**, *38*, 3157-3158.
7. T. Nishimura, T. Onoue, K. Ohe and S. Uemura, *J. Org. Chem.*, **1999**, *64*, 6750-6755.
8. T. Hosokawa and S.-I. Murahashi, *Acc. Chem. Res.*, **1990**, *23*, 49-54.
9. J. Muzart and J. P. Pete, *J. Mol. Catal.*, **1982**, *15*, 373-376.
10. S. Chowdhury, I. Rivalta, N. Russo and E. Sicilia, *J. Chem. Theory Comput.*, **2008**, *4*, 1283-1292.
11. M. J. Filatov, E. P. Talsi, O. V. Gritsenko, G. M. Zhidomirov and K. I. Zamaraev, *J. Chem. Soc. Dalton Trans.*, **1990**, 3265-3269.
12. N. R. Conley, L. A. Labios, D. M. Pearson, C. C. L. McCrory and R. M. Waymouth, *Organometallics*, **2007**, *26*, 5447-5453.
13. Spartan 06 Pro, Wvfunction, Inc., 18401 Von Karman Avenue, Suite 370, Irvine, CA 92612, USA.
14. R. Silaghi-Dumitrescu and C. E. Cooper, *Dalton Trans.*, **2005**, *21*, 3477-3482.
15. M. Surducan, S. V. Makarov and R. Silaghi-Dumitrescu, *Eur. J. Inorg. Chem.*, **2014**, *34*, 5827-5837.
16. A. A. A. Attia, A. Lupan and R. Silaghi-Dumitrescu, *RSC Adv.*, **2013**, *3*, 26194-26204.
17. R. Silaghi-Dumitrescu, *Struct. Bond.*, **2013**, *150*, 97-118.
18. R. Silaghi-Dumitrescu and I. Silaghi-Dumitrescu, *J. Inorg. Biochem.*, **2006**, *100*, 161-166.
19. R. Silaghi-Dumitrescu, I. Silaghi-Dumitrescu, E. D. Coulter and D. M. Kurtz, Jr, *Inorg. Chem.*, **2003**, *42*, 446-456.
20. R. Silaghi-Dumitrescu, *J. Biol. Inorg. Chem.*, **2004**, *9*, 471-476.
21. R. Silaghi-Dumitrescu, *Proc. Rom. Acad.*, **2004**, *3*, 149-154.
22. J. M. Keith, R. J. Nielsen, J. Oxgaard and W. A. Goddard, *J. Am. Chem. Soc.*, **2005**, *127*, 13172-13182.
23. R. H. Crabtree, "Hydride complexes of the transition metals", *Encyclopedia of Inorganic Chemistry*, 2008, p. 1527-1534.
24. L. Brammer, J. A. K. Howard, O. Johnson, T. F. Koetzle, J. L. Spencer and A. M. Stringer, *J. Chem. Soc., Chem. Commun.*, **1991**, 241.
25. R. H. Morris, *Inorg. Chem.*, **1992**, *31*, 1471.
26. Gaussian 09, Revision A.1, M. J. Frisch, G. W. Trucks, H. B. Schlegel, G. E. Scuseria, M. A. Robb, J. R. Cheeseman, G. Scalmani, V. Barone, B. Mennucci, G. A. Petersson, H. Nakatsuji, M. Caricato, X. Li, H. P. Hratchian, A. F. Izmaylov, J. Bloino, G. Zheng, J. L. Sonnenberg, M. Hada, M. Ehara, K. Toyota, R. Fukuda, J. Hasegawa, M. Ishida, T. Nakajima, Y. Honda, O. Kitao, H. Nakai, T. Vreven, J. A. Montgomery, Jr., J. E. Peralta, F. Ogliaro, M. Bearpark, J. J. Heyd, E. Brothers, K. N. Kudin, V. N. Staroverov, R. Kobayashi, J. Normand, K. Raghavachari, A. Rendell, J. C. Burant, S. S. Iyengar, J. Tomasi, M. Cossi, N. Rega, J. M. Millam, M. Klene, J. E. Knox, J. B. Cross, V. Bakken, C. Adamo, J. Jaramillo, R. Gomperts, R. E. Stratmann, O. Yazyev, A. J. Austin, R. Cammi, C. Pomelli, J. W. Ochterski, R. L. Martin, K. Morokuma, V. G. Zakrzewski, G. A. Voth, P. Salvador, J. J. Dannenberg, S. Dapprich, A. D. Daniels, Ö. Farkas, J. B. Foresman, J. V. Ortiz, J. Cioslowski, and D. J. Fox, Gaussian, Inc., Wallingford CT, **2009**.